RSC Advances




ROYAL SOCIETY OF CHEMISTRY

www.rsc.org/advances

Journal Name

ARTICLE

# New Sterically Hindered Tin(IV) Siloxane Precursors to Tinsilicate Materials: Synthesis, Spectral, Structural and Photocatalytic Studies†‡

Received 00th January 20xx,
Accepted 00th January 20xx

DOI: 10.1039/x0xx00000x

www.rsc.org/

Mohan Gopalakrishnan[a] and Nallasamy Palanisami[*a]

A series of sterically hindered tin(IV) siloxanes were synthesized by the reaction between tris(*tert*-butoxy)silanol/triphenylsilanol and orgnotin chlorides {[($^t$Bu)$_2$Sn(OSi(O$^t$Bu)$_3$)$_2$] (**1**), [($^t$Bu)$_2$Sn(OSi(O$^t$Bu)$_3$)Cl] (**2**), [(*n*-Bu)$_2$Sn(OSi(O$^t$Bu)$_3$)$_2$] (**3**), [(*n*-Bu)$_2$Sn(OSi(O$^t$Bu)$_3$)Cl] (**4**), [(Me)$_2$Sn(OSi(O$^t$Bu)$_3$)$_2$] (**5**), [(Me)$_2$Sn(OSi(O$^t$Bu)$_3$)Cl] (**6**), [($^t$Bu)$_2$Sn(OSiPh$_3$)$_2$] (**7**), [($^t$Bu)$_2$Sn(OSiPh$_3$)Cl] (**8**) whereas $^t$Bu = tertiary butyl; *n*-Bu = butyl; Me = methyl}. All the compounds were characterized by analytical and spectroscopic (FT-IR and $^1$H, $^{13}$C, $^{29}$Si, $^{119}$Sn NMR) methods. The compounds **1** and **7** were structurally characterized by single-crystal X-ray crystallography. The coordination geometry of tin ($SnO_2C_2$) is slightly distorted from tetrahedral due to sterically crowed ligands around the tin atom. In order to convert tinsilicate materials, compounds **1** and **3** were selected for thermolysis to give the identical $SnO_2.2SiO_2$ materials at low temperature (~350 °C). The degradation was investigated by thermal analysis (TGA/DTA), both compounds are having butyl groups which facile eliminate to butene gas *via* β-hydride elimination process (~250 °C). The moleuclar route to oxide materials at low temperature decribed here represents an alternative to the sol-gel technique. The tinsilicate material was examined by several techniques including infrared, powder X-ray diffraction analysis (PXRD), scanning electron microscopy (SEM) and energy dispersive X-ray (EDX). The optical band gap of material have been studied by UV–vis–NIR spectroscopy and as a result of the low band gap value ($E_g$ = 2.549 eV) due to the silicon oxide mixed with tin oxide. The prepared material act as photocatalyst for the degradation of methylene blue (MB).

## Introduction

The metallasiloxanes have attracted great interest owing to their role as model compounds for modified silica surfaces (M–O–Si), attractive physical properties, catalyst and potential precursors for new inorganic materials.[1-3] The existence of metal in the siloxane framework often results in high thermal stability and catalytic properties. It can be derived from silanol ($R_3SiOH$), silanediol ($R_2Si(OH)_2$) and silanetriol ($RSi(OH)_3$).[4-6] Moreover, these metallasiloxanes are used for synthesis of metal silicate materials.[7] The innovative materials with tailored properties often required low-temperature methods to allow the establishment of multi-metal oxide system. A synthetic approach which allows specific control over the buildup of a solid-state structure, at the atomic level has become an important objective in materials science.[8, 9] On the other hand, tin oxide is a *n*-type wide band gap (~4.0 eV) semiconductor in thin film form and its electrical properties critically depend on its oxygen stoichiometry, nature, amount of impurities or dopants present and mixed metal oxide structure shape. The progress in silicon mixed tin oxides has attracted recent interest in exploiting these materials as elements for light emitting devices.[10] Various methods have been employed for preparing doped and undoped $SnO_2$ heterostructures such as sputtering, twin polymerization and spray pyrolysis.[11] These heterojunction materials are ($SnO_2/TiO_2$, $SnO_2/ZnO$)[12, 13] used as photocatalyst for complete removal of the toxic chemicals from the industrial waste water. When such a material was irradiated with UV-light, valence band electrons are excited to conduction band with the simultaneous generation of the same amount of the holes in the valence band. In these holes and electrons are accessible for selective oxidation and reduction processes.[14] For multicomponent systems such as metal oxide materials, a major challenge in the development of sol-gel type processes is to keep homogeneity throughout the network-forming reactions. To overcome the difficulties single source precursor is focused on fine-tuning the thermolysis of the metallasiloxanes precursors.[15, 16]

Our interest in this area is focused on tinsiloxanes. The second heavy element of tin into the structure of siloxanes is motivated by the possibility to develop the potential precursor to silica support tin oxide. The thermolytic precursor approach can leads to formation of homogeneous materials from thermolysis of Sn-$(R)_4$/Si$(OR')_4$ mixtures, to achieve the high degree of homogeneity

[a]*Materials Chemistry Division, School of Advanced Sciences, VIT University, Vellore 632 014, Tamil Nadu, India.*
** Corresponding author: E-mail: palanisami.n@gmail.com; Tel: +91 98426 39776; Fax no: +91416224 3092.*

† Electronic Supplementary Information (ESI) available: CCDC 980359 (**1**), 1049393 (**2**) contain the supplementary crystallographic data for this paper. These data can be obtained free of charge from the Cambridge Crystallographic Data Centre via http://www.ccdc.cam.ac.uk/data_request/cif.

‡ This article is dedicated to Professor R. Murugavel for his contribution to the main group chemistry.

DOI: 10.1039/x0xx00000x

at low temperature. We have been examining metallasiloxanes precursor compounds that undergo thermolytic conversions at low temperature (~350 °C) to give metal silicate materials. There are few reports in literature for single source precursors to metal silicate materials. Tilley and co-workers have synthesized main group and transition metal siloxanes $M[OSi(O^tBu)_3]_n$ and their thermolytic degradation of $MO_2.nSiO_2$ materials.[17-19] Driess et al. reported the indium siloxanes to indium silicate materials and their thin film applications.[20] Recently, Bohra et al. reported the glycol modified titanium and zirconium siloxanes and their thermal conversion of silicate materials.[21] However, to the best of our knowledge, the tin siloxanes precursors and their material conversion are unknown. We herein report the synthesis, spectral characterization of tin(IV) siloxanes **1**-**8** and X-ray structure determination of two of these derivatives. We wish to select **1** and **3** represent as precursors, especially these compounds have butyl group which is facile removal of butene gas *via* β-hydride elimination at low temperature (~250 °C) to form tinsilicate materials and their spectral and photocatalytic properties were studied.

## Results and discussion

### Synthesis and spectral properties

The synthesis of organotin siloxanes **1**-**8** were carried out by using schlenk technique through reaction of one equivalent of $R_2SnCl_2$ (R = $^t$Bu, *n*-Bu, Me) with an equal or two molar ratios of $(^tBuO)_3OSiONa/Ph_3SiOH$ in benzene at room temperature (scheme 1). The compounds could be obtained as pure form after recrystallization from benzene and hexane and it is fairly thermal, moisture and air-stable colourless solids in moderate yield. Compounds are readily soluble in all non-polar organic solvents. The tin(IV) siloxanes were characterized by FT-IR, NMR spectroscopy and elemental analysis. Further the molecular structure of **1** and **7** were confirmed by single crystal X-ray diffraction studies.

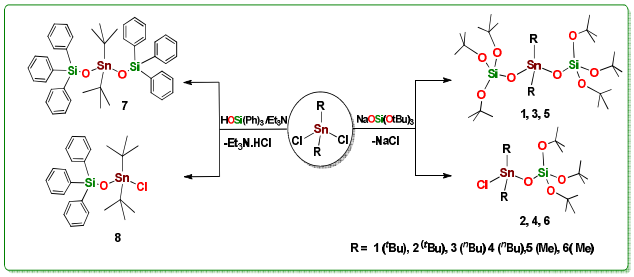


**Scheme 1**. Synthesis of tin(IV) siloxanes **1**–**8**

The $^1$H NMR spectra of compound **1**–**6** in $CDCl_3$ and $C_6D_6$ show only one singlet at δ =1.45 ppm due to the *tert*-butyl[22, 16, 17] groups of the siloxy ligands. Other singlet δ = 1.29 ppm (**1**), δ = 1.45 ppm (**2**), δ = 0.70 ppm (**5**), δ = 0.68 ppm is corresponding to the methyl groups[23, 24] around tin and the multiplets around δ = 1.71–1.79 ppm (**3**), δ = 1.60–1.88 ppm (**4**), δ = 0.91-1.00 ppm (**4**) is due to the methylene group of butyl.[25] The $^1$H NMR spectra of **7** and **8** display two singlet at δ = 0.99 and δ = 1.05 ppm for the *tert*-butyl groups of tin metal. The multiplets around δ = 7.16-7.28 and δ = 7.53-7.55 ppm (**7**) and δ = 7.16-7.28 and 7.85-7.89 ppm (**8**) corresponding to the aromatic proton of triphenyl siloxy ligand.[26, 27] The $^{13}$C NMR spectra of **1**–**6** show resonance around δ = 30 and 72 ppm, is corresponding to the *tert*-butyl group of siloxy ligands. The resonance between δ = 29.62-31.43 ppm can be assigned to the tin attached carbon (SnC) in **1**–**4**.[23, 25] Tin attached methyl carbon shows δ = 13.37 ppm (**5**) and 13.71 ppm (**6**). The $^{13}$C NMR spectra of **7** and **8** show four resonances with nearly similar chemical shifts at δ = 29.62 and 38.87 ppm (**7**) and δ = 27.87 and 38.69 ppm (**8**) respectively for *tert*-butyl group.[28] The aromatic carbon resonance between δ = 128.26–137.60 ppm (**7**) and δ = 127.48–138.23 ppm (**8**). The $^{119}$Sn chemical shift values for compounds **1**, **3** and **5** were similar (δ = -149.60 ppm, -148.98 ppm, and -151.31ppm)[29-31] and suggest similar virtual coordination geometries around the tin atom which can be compared with literature values.[34] The $^{29}$Si chemical shift values for *tert*-butoxy silanol analogues (**1**–**6**) are similar (δ = -93.60, -93.7, -92.09, -91.62, -91.36 and -91.32 ppm)[30-32] whereas the chemical shift values of aryl siloxy tin compounds are δ = -20.13 and -20.01 ppm (Table S1). Notable changes become apparent when alkoxy group is replaced by aryl group due to the alkoxy silicon atom surrounded by four electrons-rich oxygen atoms which can appear more upfield than the aryl silanol. The NMR ($^1$H, $^{13}$C, $^{29}$Si and $^{119}$Sn) spectra of compounds **1**-**8** were shown in supporting information (Fig. S4-S28).

In addition, the FT-IR spectra of compounds **1**–**7** show the sharp absorption around 2955-2980 $cm^{-1}$ due to the corresponding aliphatic C–H vibrations[35] of alkyl group in a tin (Fig. S29-31) and the alkoxy ligands whereas the band at 3064-3066 $cm^{-1}$ is due to aromatic C–H stretching (**7**, **8**) of corresponding arylsiloxy ligands. The strong infrared band appears around 960-1000 $cm^{-1}$ is Sn–O–Si linkage vibrations.[36, 22]

### Crystallography

The X-ray quality single crystals of **1** were obtained by crystallization from hexane at 10 °C temperature. The crystal structure of **1** is shown in Fig. 1 and it is crystallizes monoclinic system with four molecules per unit cell in *P121/n1* space group. With two mirror planes (Si–O) and rotation axis deceptive in the **1** possesses molecular $C_{2v}$ symmetry which is related with known main group siloxanes.[22, 37-39]

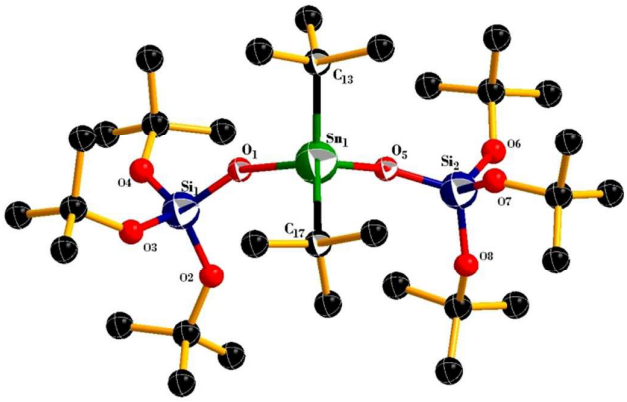


**Figure 1.** Molecular structures of $[(^tBu)_2Sn(OSi(O^tBu)_3)_2]$ (**1**). Thermal ellipsolids are drawn at the 50% probability level (the hydrogen atoms are omitted for clarity).

The coordination geometry around tin is slightly distorted from the tetrahedral due to non-bonding steric interactions of hindered ligands. The siloxy group of O1 and their symmetry equivalent of other siloxy group at O5, generated by the *tert*-butyltin axis, have a distance of 3.417 Å from each other, similarly the two *tert*-butyl group C13–C17 distance is 3.832 Å from each other, which indicates the steric interactions.[20] The two Sn–O bond lengths are almost equal (Sn–O1 = 1.948 Å and Sn–O5 = 1.966 Å) and comparable to the values of related structures.[40] The O1–Sn–O5 and C17–Sn–C13 angles are 100.85(18); 122.6(2) in **1** notably from the distorted tetrahedral angles, whereas the C13–Sn–O1 and C13–Sn–O5 bond angles are 104.3(2); 104.9(2) fairly close to it.[41] Thus, the central metal atom of tin ($SnO_2C_2$) has distorted tetrahedral coordination geometry. The both Si atoms are coordinated with slightly distorted tetrahedral geometry and each Si bond to four oxygen atoms with angles are O1–Si1–O3 112.7(2), O1–Si1–O4 111.6(2), O1–Si1–O2 106.1(2) and the other Si2 atom O5–Si2–O8 113.4(3), O5–Si2–O6 113.1(2), O5–Si2–O7, 106.4(2) respectively. The above mentioned steric interactions are due to the siloxy and *tert*-butyl ligands. These tri(*tert*-butyl)siloxy ligands are arranged in eclipsed fashion and crystal packing pattern as shown in Fig. S1.

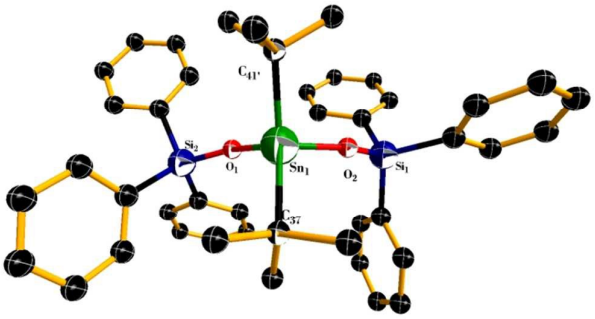


**Figure 2.** Molecular structures of $[(^tBu)_2Sn(OSiPh_3)_2]$ (**7**). Thermal ellipsolids are drawn at the 50% probability level (the hydrogen atoms are omitted for clarity).

Single crystals of **7** were obtained from benzene at room temperature. The crystal structure of **7** is shown in Fig. 2. Compound **7** crystallizes orthorhombic with four molecules per unit cell in *Pbca* space group. The central metal atom of tin ($SnO_2C_2$) has distorted tetrahedral coordination geometry. The angles are O1–Sn–O5 101.0(10)°, C41–Sn1–C37 118.9(2)° and O1–Sn1–C37 111.90(13)° which are deviated from tetrahedral angle 109.5°. It is evident that the tin atom around the crowded *tert*-butyl and –$OSiPh_3$ siloxy ligands. The Si atoms also slightly distorted tetrahedral geometry with angles are O2–Si1–C1 107.9(6), O1–Si1–C31 112.5(2); O1–Si2–C31 112.5(2), C31–Si2–C25 107.1(8). Thus, compound **7** structural features are comparable to **1**.

**Thermal degradation of 1 and 3**

The pyrolytic conversion of siloxanes to tinsilicate material was investigated by thermal analysis. The compounds have been undergo clean removal of isobutene *via* β-hydride elimination[41] and water at low temperature (250-350 °C) to give tinsilicate materials as shown in scheme 2. It is similar to reported in the literature of the main group and transition metal siloxanes to metal silicate materials.[5, 17-19]

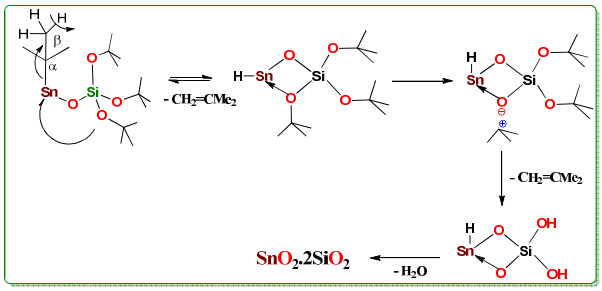


**Scheme 2**. Thermal degradation pathway of tin(IV) siloxane (**1**).

TG curve of **1** obtained at a heating rate of 10 K/min/700 °C under $N_2$ atmosphere is illustrated in Fig. 3. The estimated weight loss percentage was calculated based on the molecular formula of the compound **1**. The thermolytic conversion process occurred in a stepwise fashion. The TG curve shows first weight loss of 20.38% at 121.61 °C which indicates the removal of *tert*-butyl group attached to tin atom. The second weight loss occurs at 211 °C (49.75%) corresponding to the removal of siloxy ligands. The both weight loss indicates the removal of isobutene gas.[22] The third stage maximum rate of weight loss at 369.09 °C due to the elimination of water molecules resulting in 31% ceramic yield ($SnO_2.2SiO_2$).

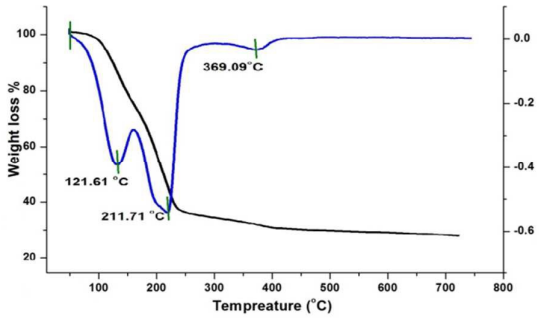


**Figure 3.** TGA and DTA curves for the degradation of **1** in $N_2$ with a heating rate of 10 K $min^{-1}$

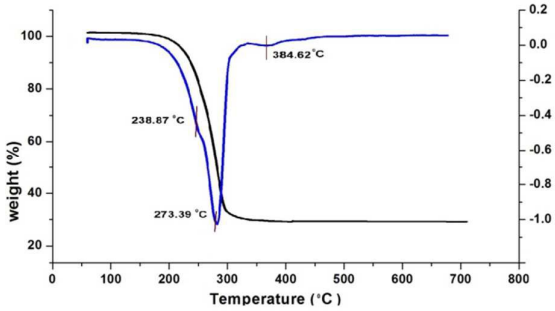


**Figure 4.** TGA and DTA curves for the degradation of **3** in $N_2$ with a heating rate of 10 K $min^{-1}$

The degradation process of **3** is slightly different from the compound **1**. TG curve show weight loss continues from 88-274 °C at which point a ceramic yield 32% (theoretical yield of expected tinsilicate 34.29%). The TGA/DTA curves suggest the thermal decomposition of **3** also three step process (Fig. 4). It takes place between 88 and 385 °C with a maximum weight loss at 274 °C resulting in an overall weight loss of 69.53%. Tinsilicate was

obtained by sintered compound **1** and **3** at 400 °C for 6 hrs in a muffle furnace to give amorphous tinsilicate materials.

**Characterization of tinsilicate material**

The FT-IR spectrum (Fig. 5) of tinsilicate materials shows a broad band at 1041 $cm^{-1}$ and 961 $cm^{-1}$ assignable to a Sn–O–Si[36, 42] hetero-linkage together with the presence of bands at 586 $cm^{-1}$ and 796 $cm^{-1}$ attributable to Sn–O and Si–O respectively. In addition, when compared with precursor compound **1** (Fig. S28) there is no peaks were observed in range of 4000-1050 $cm^{-1}$ in prepared tinsilicate materials due to the absence of carbon.

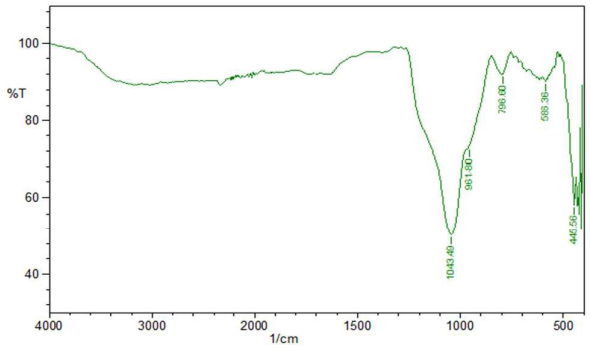


**Figure 5**. FT-IR spectrum of tinsilicate material obtained form thermolysis of **1**.

The X-ray powder diffraction patterns of tinsilicate materials obtained from degradation of compound **1** and **3**. Both are identical spectrum and the compound **1** is depicted in Fig. S33. All the diffracted peaks of tinsilicate material were shown that obtained materials are essentially amorphous. The crystallinity of materials depends on the calcinations temperature. It can be compared with the reported Al, In, Ti and Zr silicate materials.[18-21] In addition, the X-ray diffraction can be used as a technique for estimating the degree of crystallinity. The Scherrer formula used to calculate the crystallite size of prepared tinsilicate materials.[43]

$$D = 0.89 \times \lambda/\beta(\cos\theta) \quad (1)$$

Where D is the size of the crystallites, β is the full-width at half maximum and θ is the Bragg angle. The average crystallite size of prepared tinsilicate is 8.872 nm which indicates amorphous in nature. From the results few peaks assignable to the tetragonal phase of tin oxide, cassiterite (JCPDS No. 041-1445).

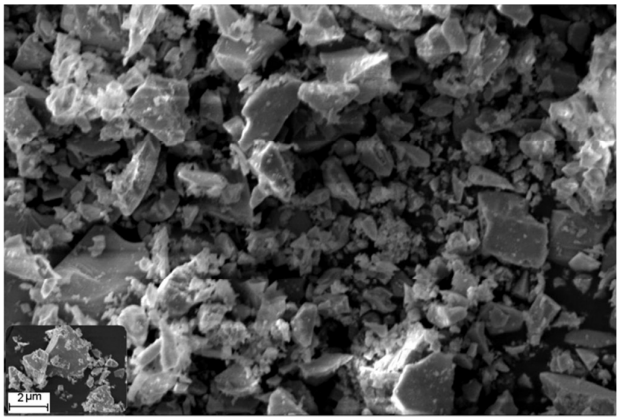


**Figure 6.** SEM images of the tinsilicate material obtained from degradation of **1**.

The scanning electron microscopic image of the homogeneous material display various sized mostly unshaped oblong particles heavily agglomerated into larger amorphous micrometer sized shapeless structures as shown in Fig. 6.

The EDX analysis of the tinsilicate was shown in Fig. 7. The composition of the tinsilicate sintered at 400 °C, it appears to indicate that the Sn/Si ratio of the mixed oxide may be controlled by the composition of the starting precursors. The molar ratio of Sn/Si is 1:2 indicating that the silicon oxide mixed in the tin framework.

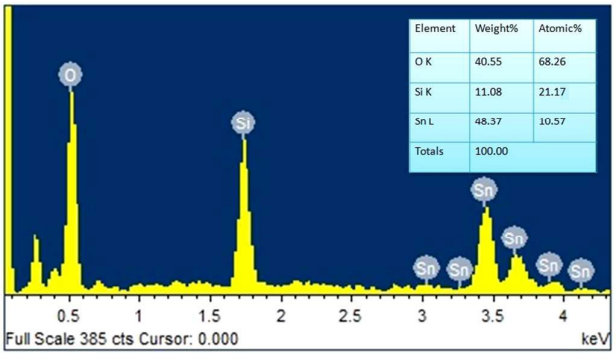


**Figure 7**. EDX analyses of the tinsilicate material obtained from degradation of **1**.

The diffused reflectance spectrum of tinsilicate material is shown in Fig. 8. The reflectance was transformed to the absorption coefficient (α) by using Kubelka-Munk equation.[44]

$$(\alpha/S) = (1-R)^2/2R \quad .....(2)$$

Where α is absorption coefficient, S is the scattering coefficient and R is the diffused reflectance at certain energy. The absorption spectra (Fig. 8a) of amorphous materials show absorption edge at 302 nm. The optical energy band gap (Eg) of highly degenerate semiconducting material was calculated the following equation.[45]

$$hv = A(hv - Eg) \quad .....(3)$$

Where A is a constant, h stands for Plank's constant and v the frequency of the incident photons.

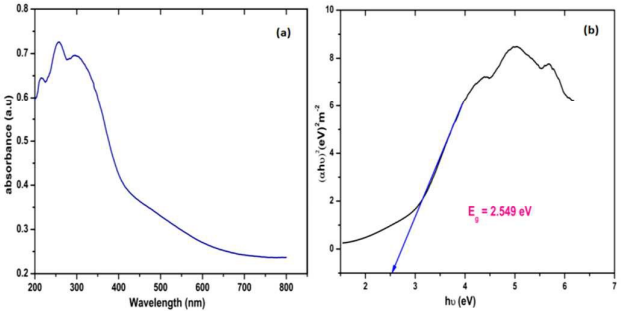


**Figure 8**. (a) UV-vis diffuse relectance spectrum; (b) Tauc's graph $[(\alpha h\upsilon)^2$ vs hυ] for calculation of band gap.

The energy band gap value was obtained from the Tauc's graph (Fig. 8b). The intersection of the line of the photon energy axis drawn from the maximum absorption end point of the curve was considered as the energy band gap ($E_g$ = 2.549 eV) of the tinsilicate

materials and the value is significantly low to commercial tin oxide ($E_g$~ 4eV)[10] which is due the silicon oxide is mixed with $SnO_2$.

**Photocatalytic activity of tinsilicate materials**

Because of the low band gap value of the tinsilicate material was suitable for a photocatalytic study for degradation of methylene blue and the experiment was performed based on the literature.[46] The most absorption peaks of MB at 665 nm (Fig. 9) decreased moderately and disappeared completely under UV light irradiation for 150 min in the presence of the tinsilicate catalyst meanwhile the colour of the solution changed gradually which indicates that the chromophoric structure of MB was degraded. The degradation capability of the tinsilicate samples was defined as $A/A_0$, where $A_0$ is the initial absorbance of methylene blue (MB) and $A$ its absorbance during the reaction. For the better understanding of photocatalytic efficiency of tinsilicate, the reaction kinetics of photodegradation MB was studied by Langmuir-Hinshelwood (L-H) kinetics model was applied as per pseudo first-order equation.[47]

$$\ln (C/C_o) = -kt \text{ ---------- (4)}$$

Here, C represents the MB at time t, and $C_o$ represents the initial MB concentration and from the plot between $\ln(C/C_o)$ and irradiation time, the degradation constant k was determined ($1.966\times10^{-2}$ $min^{-1}$) ($R^2$ = 0.97). The kinetics of photocatalytic degradation of tinsilicate materials followed the first order as shown in Fig. 9.

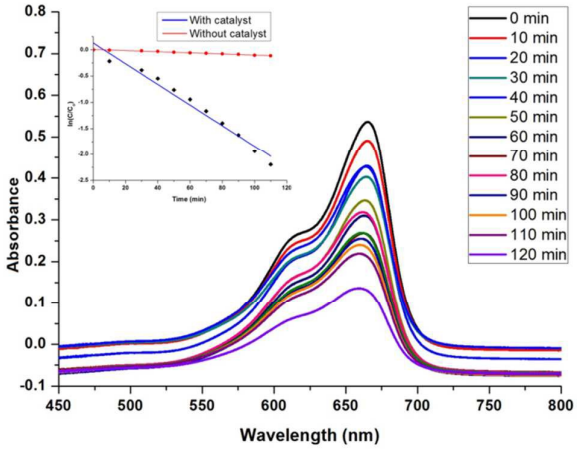


**Figure 9.** Absorbance changes of MB solution with different irradiation time in the presence of tinsilicate; Inset: Plot of $\ln(C/C_o)$ with time indicating first order kinetics.

The band gap of tinsilicate materials is 2.54 eV. It can be activated by UV light irradiation for the generation of electron-hole pairs which are responsible for the photocatalytic degradation of the organic pollutant of dyes.

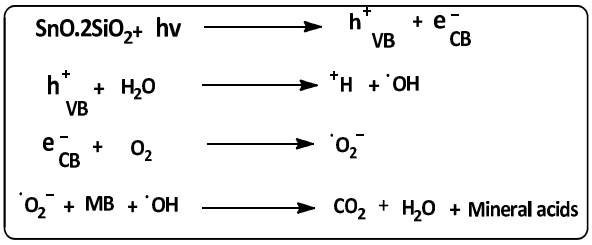


**Scheme 3**: Photodegradation pathway of methylene blue.

Under the UV light irradiation, in material electrons are excited from the valence band (VB) to conduction band (CB) called the photodegrated electrons which could react with the dissolved $O_2$ in the solution adsorbed on the surface of the photocatalyst to yield superoxide anion radical.[48] While $H^+$ reacts with the $OH^-$ to form the $^{\cdot}OH$ hydroxyl radical.[14] The MB molecule could be photodegrated *via* reaction with $^{\cdot}O_2^-$ and $^{\cdot}OH$ radical to form $CO_2$, $H_2O$ and other acids. The degradation efficiency is similar to the reference titanium oxide. The proposed degradation mechanism of tinsilicate is shown in scheme 3.

## Experimental

**Materials and methods**

All the reactions were performed under a dry nitrogen atmosphere by employing standard schlenk line techniques. Solvents were dried over sodium benzophenone ketyl and were collected from the quiet at the time of reaction. Organotin(IV) dichlorides were purchased from Alfa-Aesar was used as received. $(^tBuO)_3SiOH$ and $NaOSi(O^tBu)_3$ were prepared by literature methods.[8] $NEt_3$ purchased from Aldrich which was distilled and stored over molecular sieves. Elemental analyses were carried out using a Thermo quest CE Instruments Model EA/110 CHN elemental analyzer. $^1H$, $^{13}C$, $^{29}Si$ and $^{119}Sn$ ($C_6D_6$ and $CDCl_3$) NMR spectra were recorded on a Bruker AMX-400 MHz spectrometer. Bruker D8 advance powder X-ray diffractometer used for PXRD analysis. Infrared spectra were recorded SHIMADZU 3000 spectrometer using KBr disc cells. Thermal analyses were performed on a model Perkin Elmer STA 6000, Diamond TG/DTA thermal analyzers. The diffused reflectance spectra (DRS) were recorded on UV–vis-NIR spectrophotometer (JASCO V-670) in the wavelength range of 200-2500 nm. Microscopic analyses were performed with a zeiss SEM microscope and chemical composition analysis of the samples were carried out using energy dispersive X-ray spectroscopy (EDX) (Oxford instruments, INCA PentaFET-x3).

**Synthetic procedures**

**Procedures A**: The synthesis of tin(IV) siloxanes **1**-**6** are followed by a similar procedure. The schlenk flask was charged to a solid mixture of sodium salt of tris(*tert*-butoxy) silanol and corresponding organotin dichloride in 1:1 and/or 1:2 molar ratio in benzene solution. The reaction mixture stirred room temperature until white precipitate (NaCl) formed. Filter off the solution, volatile was removed under vacuum and the remaining white solid was extracted with dry hexane. The resulting solution was filtered and the solvent was removed by vacuum to give pure white solid as compounds. Further, the obtained compounds were purified by recrystallization using hexane and benzene.

**Synthesis of $(^tBu)_2Sn(OSi(O^tBu)_3)_2$ (1)**: Reaction of di-*tert*-butyltin dichloride (0.304 g, 1 mmol) and sodium salt of tris(*tert*-butoxy) silanol (0.573 g, 2 mmol) attended procedure A manner to afford the product as a white solid of compound **1**. Yield 63%. M.p. 44 °C. Calcd. $C_{32}H_{72}O_8Si_2Sn$ (M.w. 759.77): C, 50.17; H, 9.24%; Found: C, 50.33; H, 9.39%. $^1H$ NMR (400MHz, $CDCl_3$, TMS): δ = 1.40 ppm (s, 18H, $(C(CH_3)_3)$); 1.29 ppm (s, 54H, $(OC(CH_3)_3)$; $^{13}C$ NMR (400 MHz, $CDCl_3$, TMS): δ= 29.62 ppm (SnC); 31.56 ppm $(OC(CH_3)_3)$; 38.87 ppm

($C(CH_3)_3$); 71.72 ppm ($OC(CH_3)_3$); $^{29}$Si NMR ($CDCl_3$, TMS): -93.60 ppm; $^{119}$Sn NMR ($C_6D_6$, TMS): -149.60 ppm. FT-IR (KBr, $cm^{-1}$): 2972m, 2929m, 2852m, 1471s, 1388s, 1361s, 1240s, 1043s, 1020s, 972s, 914m, 827s, 804m, 702s, 650m, 540m.

**Synthesis of ($^t$Bu)$_2$Sn(OSi(O$^t$Bu)$_3$)Cl (2)**: Reaction of di-*tert*-butyltin dichloride (0.304 g, 1 mmol) and sodium salt of tris(*tert*-butoxy) silanol (0.287 g, 1 mmol) attended procedure A manner to afford the product as a white solid compound **2**. Yield 48%, M.p. 53 °C. Calcd. $C_{20}H_{45}ClO_4SiSn$ (M.w. 532.18): C, 45.17; H, 8.53%; Found: C, 44.96; H, 8.17%.$^1$H NMR (400MHz, $C_6D_6$, TMS): δ = 1.47 ppm (s, 18H, ($C(CH_3)_3$); 1.45 ppm (s, 27H, ($OC(CH_3)_3$); $^{13}$C NMR (400 MHz, $C_6D_6$, TMS): δ = 28.04 ppm (SnC); 30.53 ppm ($OC(CH_3)_3$); 37.77 ppm ($C(CH_3)_3$); 70.95 ppm ($OC(CH_3)_3$); $^{29}$Si NMR ($C_6D_6$, TMS): -93.37 ppm; $^{119}$Sn NMR ($C_6D_6$, TMS): -149.54 ppm. FT-IR (KBr, $cm^{-1}$): 2976m, 2920m, 2849m, 1455s, 1334s, 1386s, 1368s, 1234s, 1125s, 1031s, 1016s, 976s, 874m, 705s, 652s, 539m.

**Synthesis of (*n*-Bu)$_2$Sn(OSi(O$^t$Bu)$_3$)$_2$ (3)**: Reaction of di-butyltin dichloride (0.304 g, 1 mmol) and sodium salt of tris(*tert*-butoxy) silanol (0.573 g, 2 mmol) attended procedure A manner to afford the product as a white solid of compound **3**. Yield 65%. M.p. 50 °C. Calcd. $C_{32}H_{72}O_8Si_2Sn$ (M.w. 759.79): C, 50.59; H, 9.55%; Found: C, 50.37; H, 9.32%. $^1$H NMR (400MHz, $C_6D_6$, TMS): δ = 0.96-1.00 ppm (t, 6H, *J* = 14.4, -$CH_3$); 1.85-1.88 ppm (t, 4H, *J* = 13.2, $SnCH_2$); 1.56-1.60 ppm (m, 4H, -CH2-); 1.47 ppm (s, 54H, ($OC(CH_3)_3$) ; $^{13}$C NMR (400 MHz, $C_6D_6$, TMS): δ = 27.16 ppm (SnC); 21.44 ppm (-CH2-); 31.72 ppm; 72.67 ppm ($O(C(CH_3)_3)$); 13.75 ($CH_3$); $^{29}$Si NMR ($C_6D_6$, ppm, TMS): -90.09 ppm; $^{119}$Sn NMR ($C_6D_6$, TMS): -148.98 ppm. FT-IR (KBr, $cm^{-1}$): 2970m, 2927m, 2852m, 1469s, 1388s, 1388s, 1361s, 1238s, 1190s, 1043s, 1020s, 972s, 912w, 879w, 827m, 804w, 702s, 650m, 538m, 516m.

**Synthesis of (*n*-Bu)$_2$Sn(OSi(O$^t$Bu)$_3$)Cl (4)**: Reaction of di-butyltin dichloride (0.304 g, 1 mmol) and sodium salt of tris(*tert*-butoxy) silanol (0.286 g, 1 mmol) attended procedure A manner to afford the product as a white solid compound **4**. Yield 52%. M.p. 48 °C. Calcd. $C_{20}H_{45}ClO_4SiSn$ (M.w. 531.18): C, 45.17; H, 8.53%; Found: C, 44.92; H, 8.31%. $^1$H NMR (400MHz, $CDCl_3$, TMS): δ = 0.89-0.95 ppm (t, 6H, *J* = 16.8, -$CH_3$); 1.73-1.77 ppm (t, 4H, *J* = 15.2, $SnCH_2$), 1.33-1.43 ppm (m, 4H, -$CH_2$-), 1.28 ppm (s, 27H, ($OC(CH_3)_3$); $^{13}$C NMR (400 MHz, $CDCl_3$, TMS): δ = 26.59 ppm (SnC); 21.08 ppm (-$CH_2$-); 26.85 ppm (-$CH_2$-); 31.51 ppm; 72.88 ppm ($O(C(CH_3)_3)$); $^{29}$Si NMR ($C_6D_6$, TMS): -91.62 ppm. $^{119}$Sn NMR ($C_6D_6$, TMS): -150.23 ppm. FT-IR (KBr, $cm^{-1}$): 2973m, 2928m, 2851m, 1472s, 1386s, 1358s, 1239s, 1045s, 1021s, 972s, 913m, 823w, 802m, 703s, 652m, 541m.

**Synthesis of (Me)$_2$Sn(OSi(O$^t$Bu)$_3$)$_2$ (5)**: Reaction of di-methyltin dichloride (0.220 g, 1 mmol) and sodium salt of tris(*tert*-butoxy) silanol (0.573 g, 2 mmol) attended procedure A manner to afford the product as a white solid of compound **5**. Yield 74%. M.p. 42 °C. Calcd. $C_{26}H_{60}O_8Si_2Sn$ (M.w. 675.53): C, 46.22; H, 8.45%; Found: C, 45.98; H, 8.28%. $^1$H NMR (400MHz, $C_6D_6$, TMS): δ = 0.70 ppm (s, 6H, ($Sn(CH_3)_2$); 1.42 ppm (s, 54H, ($OC(CH_3)_3$; $^{13}$C NMR (400 MHz, $C_6D_6$, TMS): δ = 13.37 ppm (SnC); 30.81 ppm; 71.72 ppm ($OC(CH_3)_3$); $^{29}$Si NMR ($C_6D_6$, ppm, TMS): -91.33 ppm; $^{119}$Sn NMR ($C_6D_6$, ppm, TMS): -151.31 ppm (s). FT-IR (KBr, $cm^{-1}$): 2974s, 2918m, 1469s, 1390s, 1363s, 1242s, 1192s, 1053s, 1041s, 1026s, 1008s, 948w, 904m, 823s, 790s, 696s, 592s, 547s, 518s.

**Synthesis of (Me)$_2$Sn(OSi(O$^t$Bu)$_3$)Cl (6)**: Reaction of di-methyltin dichloride (0.220 g, 1 mmol) and sodium salt of tris(*tert*-butoxy) silanol (0.286 g, 1 mmol) attended procedure A manner to afford the product as a white solid compound **6**. Yield 70%. M.p. 44 °C. Calcd. $C_{14}H_{33}ClO_4SiSn$ (M. w. 447.66): C, 37.56; H, 7.43%; Found: C, 37.38; H, 7.14%. $^1$H NMR (400MHz, $CDCl_3$, TMS): δ = 1.15 ppm (s, 6H, ($Sn(CH_3)_2$), 1.32 ppm (s, 27H, ($OC(CH_3)_3$; $^{13}$C NMR (400 MHz, $CDCl_3$, TMS): δ = 13.71 ppm (SnC); 31.34 ppm; 72.88 ppm ($OC(CH_3)_3$); $^{29}$Si NMR ($C_6D_6$, TMS): -91.32 ppm; $^{119}$Sn NMR ($C_6D_6$, TMS): -151.67 ppm. FT-IR (KBr, $cm^{-1}$): 2958s, 2904m, 2877m, 1470s, 1387s, 1360s, 1233s, 1215s, 1033s, 1032s, 1012s, 960m, 908m, 818m, 785s, 699s, 552s, 516m.

**Procedures B**: To a clear solution of one and/or two molar ratio of triphenyl silanol in dry $Et_2O$. Triethylamine was added at 0 °C using a plastic syringe followed by the one molar of di-*tert*-butyltin dichlo--ride in $Et_2O$ was added dropwise and reaction mixture slowly warm to room temperature and stirred until a white precipitate ($Et_3N.HCl$) formed. Filter off the solution, volatile was removed under vacuum and the remaining white solid was extracted into dry hexane. The solution was filtered and solvent was removed by vacuum to afford pure white solid as the products. Further, the obtained compounds were purified by recrystallization using benzene.

**Synthesis of ($^t$Bu)$_2$Sn(OSiPh)$_3$)$_2$ (7)**: The reaction of triphenyl silanol (0.553 g, 2 mmol) and di-*tert*-butyltin dichloride (0.304 g, 1 mmol) were reacted the above procedure B manner to afford the product as a white solid of compound **7**. Yield 72%. M.p. 69 °C. Calcd. $C_{44}H_{48}ClO_2Si_2Sn$ (M.w. 783.69): C, 67.66; H, 6.17%; Found: C, 66.43; H, 6.13%. $^1$H NMR (400MHz, $CDCl_3$, TMS): δ = 0.99 ppm (s, 18H, ($SnC(CH_3)_3$), 7.16-7.28 ppm (m, 15H, Ar-H), 7.53-7.55 ppm (m, 15H, Ar-H); $^{13}$C NMR (400 MHz, $CDCl_3$, TMS): δ = 29.62 ppm (SnC), 31.56 ppm ($C(CH_3)_3$), 38.87 ppm ($C(CH_3)_3$), 71.72 ppm; $^{29}$Si NMR ($C_6D_6$, TMS): -20.01 ppm(s). $^{119}$Sn NMR ($CDCl_3$, TMS): -151.34 ppm (s). FT-IR (KBr, $cm^{-1}$): 3066m, 2954m, 2848m, 1587m, 1465m, 1427s, 1303s, 1259s, 1184s, 1166s, 1105s, 1066s, 1033s, 997s, 962s, 854s, 833s,740s, 696s, 621s, 505s.

**Synthesis of ($^t$Bu)$_2$Sn(OSiPh)$_3$)Cl (8)**: The reaction of triphenyl silanol (0.27g, 1 mmol) and di-*tert*-butyltin dichloride (0.152 g, 1 mmol) were reacted the above procedure B manner to afford the product as a white solid of compound **8**. Yield 68%. M.p. 63 °C. Calcd. $C_{26}H_{33}ClOSiSn$ (M.w. 543.79): C, 57.43; H, 6.12; Found: C, 57.11; H, 6.14. $^1$H NMR (400MHz, $C_6D_6$, TMS): δ = 1.05 ppm (s, 18H, ($SnC(CH_3)_3$), 7.15-7.23 ppm (m, 12H, Ar-H), 7.85-7.89 ppm (m, 3H, Ar-H); $^{13}$C NMR (400 MHz, $C_6D_6$, TMS): δ = 27.87 ppm (SnC), 38.69 ppm ($C(CH_3)_3$), 128.26 ppm (SiC) 134.28 ppm (6 Ar-C), 134.33 ppm (6 Ar-C), 137 ppm (3 Ar-C); $^{29}$Si NMR ($C_6D_6$, TMS): -20.03 ppm(s); $^{119}$Sn NMR ($C_6D_6$, TMS): -151.27 ppm (s). FT-IR (KBr, $cm^{-1}$): 3064m, 2974m, 2850m, 1587s, 1465s, 1427s, 1384s, 1367s, 1259s, 1165s, 1103s, 1033s, 997s, 962s, 852s, 806s, 740s, 700s, 505s.

**Photocatalytic studies**

The methylene blue (MB) was reagent grade and used as received. Photocatalytic activities of tinsilicate materials were assessed by the decomposition of MB dye. Reference experiments were performed



 

**Table 1**. Crystal data and structure refinement for **1** and **7**

| | **1** | **7** |
|---|---|---|
| Formula | $C_{32}H_{72}O_8Si_2Sn$ | $C_{44}H_{48}O_2Si_2Sn$ |
| Formula weight (g $mol^{-1}$) | 759.77 | 783.69 |
| Crystal system | Monoclinic | Orthorhombic |
| Space group | P121/n1 | Pbca |
| Crystal size (mm) | 0.57 × 0.53× 0.5 | 0.35× 0.25 × 0.20 |
| a (Å) | 9.505(2) | 18.246(7) |
| b (Å) | 16.483(4) | 20.949(7) |
| c (Å) | 27.196(6) | 21.426(8) |
| α (°) | 90.00 | 90.00 |
| β (°) | 97.697(2) | 90.00 |
| γ (°) | 90.00 | 90.00 |
| V($Å^3$) | 4222.8(1) | 8190.4(5) |
| Z | 4 | 8 |
| D calcd (Mg $m^{-3}$) | 1.195 | 1.271 |
| T (K) | 150(2) | 296(2) |
| μ ($mm^{-1}$) | 0.745 | 0.716 |
| F (0 0 0) | 1624 | 3248 |
| Number of independent reflections/Rint | 9618 | 8327 |
| Number of reflection Observed with (I > 2σ(I)) | 6136 | 5468 |
| Number of refined parameters | 412 | 479 |
| Theta(max) | 27.485 | 26.336 |
| GOF ($F^2$) | 1.118 | 1.103 |
| $R_1$ ($F$) (I > 2σ(I)) | 0.033 | 0.037 |
| | 0.039 | 0.079 |
| $wR_2$ ($F^2$) (all data) | 0.072 | 0.092 |
| | 0.075 | 0.074 |
| (Δ/σ)max | 0.001 | 0.008 |

with commercial $TiO_2$ used as a photocatalytic standard. In each experiment about 30 mg of the prepared catalyst was added to 40 ml MB aqueous solution (20 mg/L). The degradation process was observed by measuring the absorption of MB at 665 nm using UV–vis absorption spectrometer. The solution was stirred in the dark for 30 min to reach adsorption and desorption equilibrium. The photocatalytic study was carried out at room temperature under UV light irradiation from six medium pressure mercury lamps (8W 254 nm UV lamps) set in parallel to the reaction tube. Heber multilamp photoreactor (model HML-MP-88) was used for photocatalysis. In every 10 min intervals, 3 mL of the suspension were collected and then centrifuged to separate the photocatalyst particles and monitoring the absorption maximum at $\lambda_{max}$ = 665 nm of supernatant.

**Single-crystal X-ray solution and refinement**

Single crystals of **1** and **7** were obtained from benzene and hexane solution. Suitable crystals were used for the X-ray diffraction studies on a Bruker SMART APEXII diffractometer and Bruker KAPPA APEXII diffractometer respectively. The structure solution was achieved by direct methods as implemented in SHELXS-97. [49] The refinement and all further calculations were carried out using SHELXS-97.[50] Further crystallographic data and parameters are summarized in Table 1.

## Conclusions

We have described the synthesis of tin(IV) siloxanes (**1**-**8**) precursors from sterically crowded $(HOSi(O^tBu)_3/HOSi(Ph)_3$ silanols. The compound **1** and **7** were structurally characterized by the single crystal X-ray diffraction studies. The geometry of tin is distorted tetrahedral due to the sterically bulky ligands. The single-source precursors **1** and **3** were well suited for producing carbon-free tinsilicate materials with retention of the Sn/Si ratio at low temperature. It represents an alternative route to the sol-gel method. The materials were characterized by spectroscopic and microscopic techniques. The optical band gap (Eg = 2.549 eV) was calculated by diffuse reflectance method which is lower than the commercial $SnO_2$ and indicates that the silicon oxide is mixed with tin oxide. The tinsilicate act as photocatalyst for degradation of methylene blue and the efficiency is similar to the reference titanium oxide.

## Acknowledgements

We gratefully acknowledge the finical support from the DST/SERB government of India (Grant No. SR/FT/CS-11/2011). We thanks, VIT University and VIT-SIF for providing instruments and lab facilities. We also thank SAIF, IIT-Madras for providing the single crystal XRD data.

## References

1 R. Murugavel, A. Voigt, M. G. Walawalkar, H. W. Roesky, *Chem. Rev.,* 1996, **96**, 2205–2236.
2 L. King, A. C. Sullivan, *Coord. Chem. Rev.,* 1999, **189**, 19–57.
3 J. Beckmann, K. Jurkschat, *Coord. Chem. Rev.,* 2001, **215**, 267–300. (b) L. -C. Pop, M. Saito, *Coord. Chem. Rev.,* 2015, http://dx.doi.org/10.1016/j.ccr.2015.07.005.
4 (a) K. W. Terry, C. G. Lugmair, and T. D. Tilley. *J. Am. Chem. Soc.,* 1997, **199**, 9745–9756. (b) H. Schmidbaur, *Angew.Chem. Int. Ed. Engl.,* 1965, **4**, 201–211.
5 A. K. McMullen, T. D. Tilley, A. L. Rheingold, S. J. Geib, *Inorg. Chem.,* 1989, **28**, 3772–3774.
6 (a) F. J. Feher, *J. Am. Chem. Soc.,* 1986, **108**, 3850–3852. (b) Y. Iwasawa (Ed.), Tailored Metal Catalysts, Reidel, *Boston,* 1986. (c) W. Xie, H. Wang , H. Li, *Ind. Eng. Chem, Res,.* 2012, **51**, 225–231.
7 (a) F. J. Feher, T. A. Budzichowski, *Polyhedron,* 1995, **14**, 3239–3253. (b) R. Murugavel, P. Davis, and V. S. Shete, *Inorg. Chem.,* 2003, **42**, 4696–4706.
8 (a) E. A. Reyes-Garcia, F. Cervantes-Lee, K. H. Pannell, *Organometallics,* 2001, **20**, 4734–4740. (b) B. Boury, R. J. P. Corriu, R. Nunez, *Chem. Mater.,* 1998, **10**, 1795–1805.
9 (a) D. R. Uhlmann, D. R. Ulrich, Ultrastructure Processing of Advanced Materials, 1992, Wiley-Interscience. (b) D. W. Bruce, D. O'Hare, *Inorganic Materials,* 1992 Wiley VCH.
10 A. A. Yelwande, M. E. Navgire, D. T. Tayde, B. R. Arbad, M. K. Lande, *Bull. Korean Chem. Soc.,* 2012, **33**, 1856–1860.
11 (a) M. Batzill and U. Diebold, *Prog. Surf. Sci.,* 2005, **79**, 147–154. (b) P. S. Patil, *Mater. Chem. Phys.,* 1999, **59**, 185–198. (c) C.

Leonhardt, S. Brumm, A. Seifert, G. Cox, A. Lange, T. Ruffer, D.Schaarschmidt, H. Lang, N. Johrmann, M. Hietschold, F. Simon, M. Mehring, *ChemPlusChem,* 2013, **78**, 1400–1412.
12 (a) R. Zhang, H. Wu, D. Lin and W. Pan, *J. Am. Chem. Soc.,* 2009, **92**, 2463–2466. (b) C. Liu, C. Li, X. Fu, F. Raziq, Y. Qu, L. Jing *RSC Adv.,* 2015, **5**, 37275–37280.
13 (a) J. King, Q. Kuang, Z. -X. Xie, L. -S. Zheng, *J. Phys. Chem. C,* 2011, **115**, 7874–7879. (b) M. L. Zhang, T. C. An, X. H. Hu, C. Wang, G. Y. Sheng, J. M. Fu, *Appl. Catal. A,* 2004, **260**, 215–222.
14 (a) C. Wang, J. C. Zhao, X. Wang, B. Mai, G. Sheng, P. Peng, J. Fu *Appl. Catal. B,* 2002, **39**, 269–279. (b) Z. Zhang, C. Shao, X. Li, L. Zhang, H. Xue, C. Wang, Y. Liu, *J. Phys. Chem. C,* 2010, **114**, 7920–7925.
15 (a) U. J. Schubert, *Chem. Soc., Dalton Trans.,* 1996, 3343–3348. (b) U. Schubert, N. Hu sing, A. Lorenz, *Chem. Mater.,* 1995, **7**, 2010–2027.
16 K. Su, T. D. Tilley, *Chem. Mater.,* 1997, **9**, 588–595.
17 M. P. Coles, C. G. Lugmair, K. W. Terry, T. D. Tilley, *Chem. Mater.,* 2000, **12**, 122–131.
18 R. L. Brutchey, J. E. Goldberger, T. S. Koffas, T. D. Tilley, *Chem. Mater.,* 2003, **15**, 1040–1046.
19 (a) K. L. Fujdala, T. D. Tilley, In Organosilicon Chemistry V - From Molecules to Materials, N. Auner and J. Weis, Eds.; VCH, Weinheim, 2003, 379. (b) C. G. Lugmair, T. D. Tilley, *Inorg. Chem.,* 1998, **37**, 764–769.
20 (a) K. Samedov, Y. Aksu, M. Driess, *ChemPlusChem.,* 2012, **00**, 1–13. (b) M. Tsaroucha, Y. Aksu, J. D. Epping, M. Driess *ChemPlusChem.,* 2013, **78**, 62–69.
21 (a) V. Dhayal, S. M. Mobin, A. Chaudhary, P. Mathur, B. L. Choudhary, M. Nagar, R. Bohra, *Dalton Trans.,* 2012, **41**, 9439–9450. (b) V. Dhayal, M. Kumar Atal, B. L. Choudhary, M. Nagar, R. Bohra, *J. Sol-Gel. Sci. Technol.,* 2009, **52**, 97–108.
22 C. W. Terry, P. K. Ganzal, T. D. Tilley, *Chem. Mater.,* 1992, **4**, 1290–1295.
23 F. Wang, R. Zhang, S. Cheng, Q. Li, C. Ma, *J. Organomet. Chem.,* 2015, **789**, 46–52.
24 C. Ma, Q. Li, M. Guo, R. Zhang, *J. Organomet. Chem.,* 2009, **694**, 4230–4240.
25 V. Chandrasekhar, R. Thirumoorthi, *Organometallics,* 2009, **28**, 2096–2106.
26 G. A. Sigel, R. A. Bartlett, D. Decker, M. M. Olmstead, P. P. Power, *Inorg. Chem.,* 1987, **26**, 1773–1780.
27 S. P. Qiu, R. Cheng, B. Liu, B. Tumanskii, R. J. Batrice, M. Botoshansky, M. S. Eisen, *Organometallics,* 2011, **30**, 2144–2148.
28 (a) B. J. Brisden, M. F. Mahon, C. C. Reinford, *J. Chem. Soc. Dalton Trans.,* 1998, 3295–3300. (b) M. Lazell, M. Motevalli, S. A. A. Shah, A. C. Sullivan, *J. Chem. Soc. Dalton Trans.,* 1997, 3363–3366.
29 V. Chandrasekhar, R. Thirumoorthi, R. K. Metre, B. Mahanti, *J. Organomet. Chem.,* 2011, **696**, 600–606.
30 K. W. Terry, K. Su, T. D. Tilley, A. L. Rheingold, *Polyhedron*, 1997, **17**, 891–897.
31 K. W. Terry, C. G. Lugmair, P. K. Gantzel, and T. D. Tilley, *Chem. Mater.,* 1996, **8**, 274–280.
32 P. A. J. McManus, D. Cunningham, and M. J. Hynes, *J. Organomet*. *Chem.*, 1994, **468**, 87–92.
33 J. Beckmann, K. Jurkschat, D. Dakternieks, A. E. K. Lim, K. F. Lim, *Organometallics,* 2001, **20**, 5125–5133.
34 (a) V. I. Bakhmutov, NMR spectroscopy in liquids and solids, 2015, Taylor & Francis group CRC press. (b) D. Dakternieks, J. H. Zhu, D. Masi, C. Mealli, *Inorg. Chem.,* 1992, **31**, 3601–3606.
35 J. Beckmann, D. Dakternieks, A. Duthie, M. L. Larchin, E. R. T. Tiekink, *Appl. Organomet. Chem.,* 2003, **17**, 52–60.
36 (a) J. Beckmann, K. Jurkschat, D. Dakternieks, M. Schurmann, *J. Organomet. Chem.,* 1997, **543**, 229–232. (b) V. C. Farmer, J.D. Russell, *Spectrochim. Acta,* 1964, **20**, 1149–1173.
37 Y. Chi, T. -Y. Chou, Y. -J. Wang, S. -F. Huang, A. J. Carty, L. Scoles, K. A. Udachin, S. -M. Peng, G. -H. Lee, *Organometallics,* 2004, **23**, 95–103.
38 U. Dembowski, T. Pape, R. Herbst-Irmer, E. Pohl, H. W. Roesky, G. M. Sheldrick, *Acta Crystallogr. Sect. C,* 1993, **49**, 1307–1309.
39 M. F. Self, A. T. Mcphail, R. L. Wells, *J. Coord. Chem.,* 1993, **29**, 225–232.
40 V. Chandrasekhar, S. Nagendran, V. Baskar, *Coord. Chem. Rev.,* 2002, **235**, 1–52.
41 P. J. Davidson, M. F. Lappert, P. Pearce, *Chem. Rev*. 1976, **76**, 219–242.
42 V. Chandrasekhar, V. Baskar, A. Steiner, S. Zacchini, *Organometallics,* 2004, **23**, 1390–1395.
43 B. E. Warren, X-Ray Diffraction. Dover, New York, 1969.
44 (a) J. Tauc, R. Grigorovici, A. Vancu, *Phys. Status Solid B.,* 1966, **15**, 627–637. (b) P. P. Sahoo, P. A. Maggard, *Inorg. Chem.,* 2013, **52**, 4443–4450.
45 P. Kubelka, F. Z Munk, *Tech. Phys. (Leipzig).,* 1931, **12**, 593–601.
46 Md.T. Uddin, Y. Nicolas, C. Olivier, T. Toupance, L. Servant, M. M. Müller, H. J. Kleebe, J. Ziegler, W. Jaegermann. *Inorg. Chem.,* 2012, **51**, 7764–7773.
47 H. Huang, K. Liu, K. Chen, Y. Zhang, Y. Zhang and S. Wang, *J.Phys. Chem. C.,* 2014, **118**, 14379–14387. (b) W. Li, Y. Tian, P. Li, B. Zhang, H. Zhang, W. Geng, Q. Zhang, *RSC Adv.,* 2015, **5**, 48050–48059.
48 J. Luan, K. Ma, B. Pan, Y. Li, X. Wu and Z. Zou, *J.Mol.catal. A: chem.,* 2010, **321**, 1–9.
49 M. Sheldrick, SHELXS-97, Program for crystal structure solution,University of Göttingen, Germany, 1997.
50 G. M. Sheldrick, SHELXL-97, program for crystal structure refinement, University of Göttingen, Germany, 1997.



 

Graphical abstract